The Astrophysical Journal, 893:44 (4pp), 2020 April 10 https://doi.org/10.3847/1538-4357/ab7c5c

The Rarity of Repeating Fast Radio Bursts from Binary Neutron Star Mergers

G. Q. Zhang[1], S. X. Yi[2], and F. Y. Wang[1,3]

[1] School of Astronomy and Space Science, Nanjing University, Nanjing 210093, People's Republic of China; fayinwang@nju.edu.cn
[2] School of Physics and Physical Engineering, Qufu Normal University, Qufu 273165, People's Republic of China
[3] Key Laboratory of Modern Astronomy and Astrophysics (Nanjing University), Ministry of Education, Nanjing 210093, People's Republic of China
Received 2019 December 30; revised 2020 February 9; accepted 2020 March 2; published 2020 April 14

Abstract

Fast radio bursts (FRBs) are extragalactic, bright pulses of emission at radio frequencies with millisecond durations. Observationally, FRBs can be divided into two classes, repeating FRBs and non-repeating FRBs. At present, 20 repeating FRBs have been discovered with unknown physical origins. Localization of the first repeating FRB 121102 and discovery of an associated persistent radio source support that FRBs are powered by young millisecond magnetars, which could be formed by the core-collapses of massive stars or binary neutron star (BNS) mergers. These two formation channels can be distinguished by the gravitational waves generated by BNSs mergers. We first calculate the lower limit of the local formation rate of repeating FRBs observed by the Canadian Hydrogen Intensity Mapping Experiment (CHIME). Then we show that only a small fraction (6%) of repeating FRBs are produced by young magnetars from BNS mergers, based on the gravitational-wave detections by the third observing run (O3) of the Advanced LIGO/Virgo gravitational-wave detectors. Therefore, we believe that repeating FRBs are more likely produced by newborn magnetars newborn from the core-collapses of massive stars rather than magnetars from BNS mergers.

Unified Astronomy Thesaurus concepts: Radio transient sources (2008); Gravitational waves (678); Gamma-ray bursts (629); Magnetars (992)

1. Introduction

Fast radio bursts (FRBs) are millisecond-duration radio pulses with large dispersion measures (DMs) that exceed the Milky Way contribution along the line of sight (Cordes & Chatterjee 2019; Petroff et al. 2019; Platts et al. 2019). At present, 20 FRBs are known to show multiple bursts (Spitler et al. 2016; CHIME/FRB Collaboration et al. 2019a, 2019b; Kumar et al. 2019; Fonseca et al. 2020), indicating non-cataclysmic sources. Whether or not all FRBs are repeating sources is still under debate (Caleb et al. 2019; James 2019). The rate of non-repeating FRBs is larger than that of any known cataclysmic events, pointing to a population of repeating sources (Ravi 2019). The physical origins of FRBs are still mysterious. The observed short timescale structure in FRB light curves requires stellar-mass compact objects as central engines, such as magnetars (Popov & Postnov 2013; Kulkarni et al. 2014; Murase et al. 2016; Beloborodov 2017; Metzger et al. 2017; Margalit et al. 2018), binary neutron star (BNSs) mergers (Totani 2013; Wang et al. 2016; Yamasaki et al. 2018; Zhang 2020), and interacting models (Geng & Huang 2015; Dai et al. 2016; Zhang 2017).

The first repeating FRB source, FRB 121102, has been localized to a star-forming, dwarf galaxy at $z = 0.19$ (Chatterjee et al. 2017; Tendulkar et al. 2017). This FRB is also spatially associated with a luminous persistent radio source (Marcote et al. 2017). The properties of the host galaxy of FRB 121102 are similar to those of superluminous supernovae and long gamma-ray bursts (Metzger et al. 2017; Tendulkar et al. 2017; Zhang & Wang 2019), which supports the central engine of repeating FRBs being a young magnetar formed by the core-collapse of a massive star (Metzger et al. 2017; Margalit et al. 2018). In this scenario, the persistent radio source could be produced by emission from a compact magnetized nebula surrounding the young magnetar (Kashiyama & Murase 2017; Metzger et al. 2017; Margalit et al. 2018). Recently, three FRBs (FRBs 180924, 181112, and 190523) that have not yet been observed to repeat were localized (Bannister et al. 2019; Prochaska et al. 2019; Ravi et al. 2019). The host galaxies of these three FRBs are massive galaxies with low star formation, similar to the hosts of short gamma-ray bursts (Berger 2014). Moreover, the offsets between the bursts and host centers are about 4 and 29 kpc for FRB 180924 and FRB 190523, respectively. Therefore, the central magnetar powering FRBs may also be formed by BNS mergers (Margalit et al. 2019; Wang et al. 2020). The properties of some repeating FRBs are consistent with a scenario in which millisecond magnetars formed from a BNS merger (CHIME/FRB Collaboration et al. 2019b; Margalit et al. 2019; Wang et al. 2020). From numerical simulations, Yamasaki et al. (2018) found that a fraction of BNS mergers may leave a rapidly rotating and stable neutron star, and that this may generate repeating FRBs 1–10 yr after the merger.

The two formation channels of magnetars, i.e., core-collapse or BNS merger, can be distinguished by the rate of gravitational-wave (GW) events observed (Zhang 2014; Callister et al. 2016) by Advanced LIGO/Virgo. In this paper, we constrain the fraction of repeating FRBs from BNS mergers with gravitational-wave observations. In Section 2 we describe a robust method to calculate the lower limit of the local rate of repeating FRBs. The results are shown in Section 3. A discussion and conclusions appear in Section 4.

2. Method

We collect the data of repeating FRBs from observations with the Canadian Hydrogen Intensity Mapping Experiment (CHIME) (CHIME/FRB Collaboration et al. 2019a, 2019b; Fonseca et al. 2020), which is the largest sample of repeating FRBs observed by the same telescope. CHIME/FRB Collaboration et al. (2019a) reported the second repeating FRB 180814 discovered during the commissioning phase and CHIME/FRB Collaboration et al. (2019b) reported eight new repeating sources observed from 2018

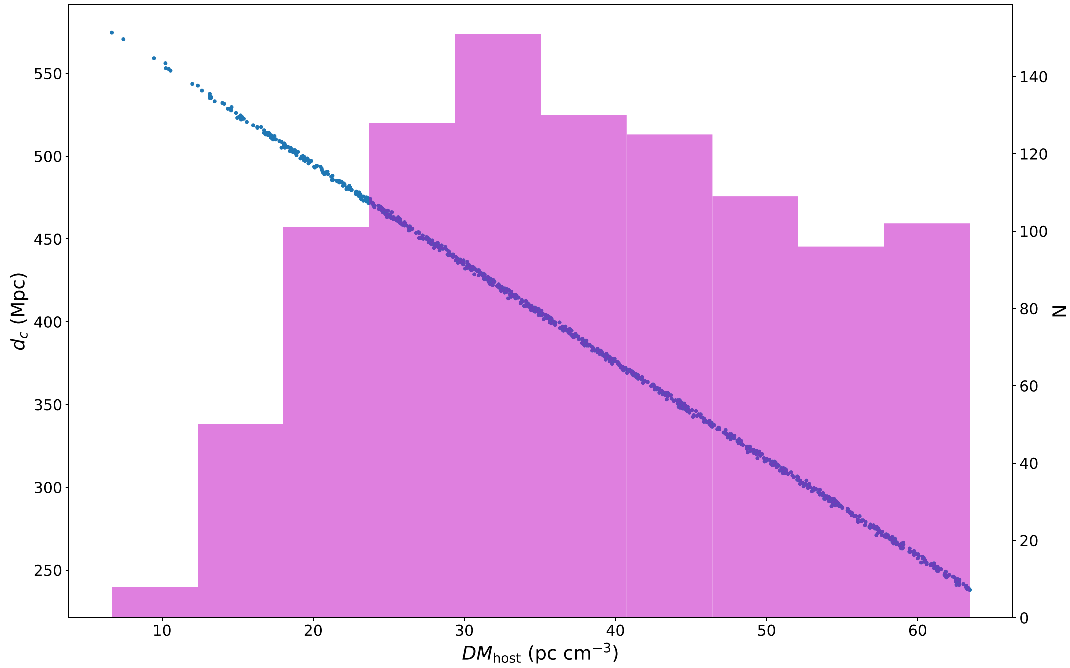

Figure 1. The pink histogram shows 1000 host galaxy dispersion measures randomly selected from 10^5 simulated host galaxy dispersion measures according to Zhang et al. (2020). The number of host galaxies is shown on the right axis. The value of $\mathrm{DM_{host}}$ satisfies $\mathrm{DM_{host}} < \mathrm{DM_{ex,lowest}}$, where $\mathrm{DM_{ex,lowest}}$ is the lowest $\mathrm{DM_{ex}}$ among repeating FRBs. In this case, only the three FRBs with the lowest $\mathrm{DM_{ex}}$ are considered. The blue scatter points represent critical distances d_c for different values of host galaxy dispersion measures. The critical distance d_c denotes the distance required to include the three FRBs with the lowest $\mathrm{DM_{ex}}$.

August 28 to 2019 March 13. Recently, nine new repeating FRBs were reported by Fonseca et al. (2020). These new FRBs were observed from 2018 August 28 to 2019 September 30. The total DM of each FRB and DM contributed by the Milky Way are given in those works. We use these data to estimate the redshifts of these repeating FRBs. In the following, we adopt the method developed by Ravi (2019) to investigate the lower limit of the formation rate.

The DMs of FRBs can be separated into different parts

$$\mathrm{DM} = \mathrm{DM_{MW}} + \mathrm{DM_{halo}} + \mathrm{DM_{IGM}} + \frac{\mathrm{DM_{host}}}{1+z}, \qquad (1)$$

where $\mathrm{DM_{MW}}$, $\mathrm{DM_{halo}}$, $\mathrm{DM_{IGM}}$, and $\mathrm{DM_{host}}$ represent the DM contributed by the Milky Way, the Milky Way halo, the intergalactic medium (IGM), and the host galaxy, respectively. In our analysis, the values of $\mathrm{DM_{MW}}$ are derived from the NE2001 model (Cordes & Lazio 2002). The $\mathrm{DM_{halo}}$ is difficult to estimate. A uniform distribution of $\mathrm{DM_{halo}}$ from 50 to 80 pc cm^{-3} is adopted in our work (Prochaska & Zheng 2019). In order to achieve a good description of $\mathrm{DM_{host}}$, we use the results of Zhang et al. (2020). They used the IllustrisTNG simulation to estimate the value of $\mathrm{DM_{host}}$ at different redshifts. $\mathrm{DM_{IGM}}$ can be calculated from (Ioka 2003; Deng & Zhang 2014)

$$\mathrm{DM_{IGM}}(z) = \frac{3cH_0\Omega_b}{8\pi G m_p} f_{\mathrm{IGM}} \int_0^z \frac{H_0 f_e(z')(1+z')}{H(z')} dz', \qquad (2)$$

where H_0 is the Hubble constant, Ω_b is baryon density, m_p is the rest mass of protons, $H(z)$ is the Hubble parameter, $f_{\mathrm{IGM}} \simeq 0.83$ is the fraction of baryon mass in the IGM (Shull et al. 2012) and

$$f_e(z') = y_1 f_{e,\mathrm{H}}(z') + y_2 f_{e,\mathrm{He}}(z') \qquad (3)$$

is the number ratio between the free electrons and baryons. In this equation, $f_{e,\mathrm{H}}(z')$ and $f_{e,\mathrm{He}}(z')$ are the ionization fractions of hydrogen and helium, respectively. $y_1 \simeq 3/4$ is the fraction of hydrogen in the universe and $y_2 \simeq 1/4$ is the helium abundance. Assuming the hydrogen and helium are fully ionized, we can get $f_e(z') \simeq 7/8$.

The CHIME observations are incomplete for FRBs with high DM values (Shull & Danforth 2018; Ravi 2019). In order to overcome this incompleteness, the local formation rate of repeating FRBs is derived from the lowest-DM CHIME FRBs, similar to the approach of Ravi (2019). The three FRBs with the lowest extragalactic dispersion measures $\mathrm{DM_{ex}}$ are chosen for analysis, where $\mathrm{DM_{ex}} = \mathrm{DM_{halo}} + \mathrm{DM_{IGM}} + \mathrm{DM_{host}}/(1+z)$. Since the chosen FRBs have very low redshifts, the effects of redshift evolution are negligible. We introduce a probability function $p(<d|\mathrm{DM_{ex}})$ to indicate the possibility that an FRB with $\mathrm{DM_{ex}}$ has the distance $d_{\mathrm{FRB}} < d$. The critical distance d_c is determined by the following criteria: the two FRBs with the lowest $\mathrm{DM_{ex}}$ have $p(<d_c|\mathrm{DM_{ex}}) \simeq 1$ and the FRB with the third-lowest $\mathrm{DM_{ex}}$ has $p(<d_c|\mathrm{DM_{ex}}) \simeq 0.95$. The probability $p(<d|\mathrm{DM_{ex}})$ can be derived from distributions of $\mathrm{DM_{host}}$, $\mathrm{DM_{halo}}$, and $\mathrm{DM_{IGM}}$. In our analysis, we assume that the distribution of $\mathrm{DM_{halo}}$ satisfies the uniform distribution between 50 and 80 pc cm^{-3} (Prochaska & Zheng 2019). The distribution of $\mathrm{DM_{IGM}}$ satisfies the standard normal distribution with a 1σ error of 10 pc cm^{-3} (Shull & Danforth 2018). According to the results of Zhang et al. (2020), we simulate 10^5 host galaxy DMs and randomly select 1000 host galaxy DMs that satisfy $\mathrm{DM_{host}} < \mathrm{DM_{ex,lowest}}$. The histogram of $\mathrm{DM_{host}}$ is shown in Figure 1. The red histogram shows the

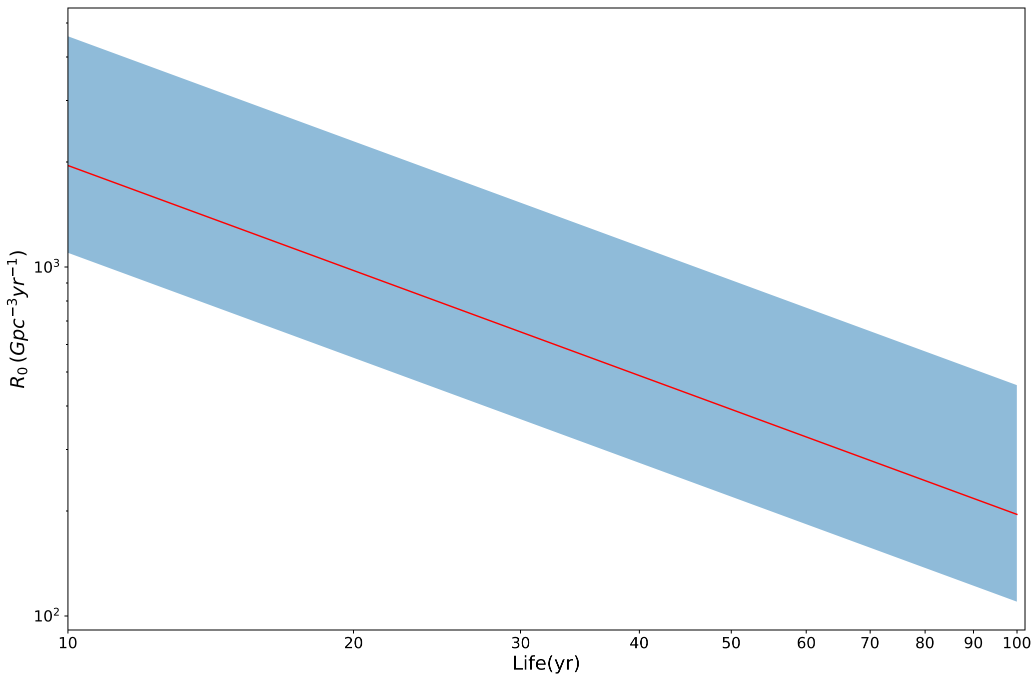

Figure 2. The red line indicates the lower limit of volumetric rate R_0 given a d_c corresponding to the three CHIME repeating FRBs with the lowest $\mathrm{DM_{ex}}$. The blue area represents the 1σ confidence level caused by the uncertainties of $\mathrm{DM_{host}}$. The beaming factor $f_b = 0.1$ is used. The lower limit of the formation rate is higher than the rate of GW events detected by aLIGO/Virgo.

distribution of $\mathrm{DM_{host}}$. Based on assumptions of $\mathrm{DM_{IGM}}$ and $\mathrm{DM_{halo}}$, we derive the critical distance d_c for different values of $\mathrm{DM_{host}}$ and show the results as blue points in Figure 1. The blue points denote the value of d_c for different host galaxy DMs. If there is no $\mathrm{DM_{host}}$ contribution, the value is $d_c \simeq 574$ Mpc. By comparison, the value of d_c is about 739 Mpc for non-repeating FRBs of CHIME without $\mathrm{DM_{host}}$ contribution (Ravi 2019).

3. Results

For the three FRBs with the lowest $\mathrm{DM_{ex}}$, we calculate the lower limit of formation rate R_0 from

$$R_0\tau = \frac{N}{V(d_c)\eta_\Omega f_b}, \tag{4}$$

where τ is the lifetime of the repeater, $N = 3$ is the number of FRBs, $V(d_c) = 4\pi d_c^3/3$ is the largest volume that contains the three FRBs, η_Ω is the sky coverage of CHIME, and f_b is the beaming factor. In this equation, we introduce the lifetime of repeaters τ. If the observation time $T_{\rm obs} \ll \tau$, the number of repeating FRBs observed in $T_{\rm obs}$ is actually the sum of repeating FRBs that burst in the past τ years. In Equation (4), the left part is the predicted number density of FRBs and the right part is the observed number density of repeating FRBs. CHIME/FRB Collaboration et al. (2019b) reported eight new repeating FRBs observed from 2018 August 28 to 2019 March 13. The latest nine repeating FRBs were observed from 2018 August 28 to 2019 September 30. The observation time is about 400 days. This observation time is so long that we can ignore the effect of the active periods of the repeating FRBs. Besides, compared with the lifetimes of repeaters, the observation time is short. Therefore, we can use Equation (4) to derive the lower limit of the formation rate. The field of view of CHIME is about 256 deg^2 (CHIME/FRB Collaboration et al. 2018), so $\eta_\Omega = 256/41242.96$. Based on the above arguments, the lower limit of the local formation rate is

$$R_0 = 1955^{+2633}_{-856} f_b^{-1}\tau^{-1}\ \mathrm{Gpc^{-3}\ yr^{-1}}. \tag{5}$$

The 1σ error comes from the uncertainty of $\mathrm{DM_{host}}$. The lifetime of a repeater significantly affects the value of R_0. The typical magnetic active timescale is 20 yr for high-mass neutron stars and 700 yr for normal-mass neutron stars (Beloborodov & Li 2016). For Galactic BNS systems, the mass distribution peaks above the maximum stable mass (Margalit & Metzger 2019). If an extragalactic population has a similar mass distribution, a large fraction of mergers will leave high-mass neutron stars. Furthermore, a merger-remnant magnetar may emit repeating bursts for about 10 yr from numerical simulation (Yamasaki et al. 2018), which is consistent with the active time of FRB 121102. Therefore, the most probable lifetime for magnetic activity is 20 yr. From the FRB 121102 observation, the constraint on the age of the central magnetar is also about a few decades (Cao et al. 2017; Kashiyama & Murase 2017; Metzger et al. 2017). Therefore, we adopt a lifetime between 10 and 100 yr. The value of f_b is not constrained observationally. We adopt a fiducial value of $f_b = 0.1$ (Nicholl et al. 2017), which is appropriate for pulsars. For illustration purposes, we calculate the local formation rate R_0 for a lifetime from 10 to 100 yr. The result is shown as the red line in Figure 2. The blue region is the 1σ confidence level. In this framework, the formation rate of repeating FRBs is

$$R_0 \sim \begin{cases} 1955\ \mathrm{Gpc^{-3}\ yr^{-1}},\ \tau = 10\ \mathrm{yr} \\ 195\ \mathrm{Gpc^{-3}\ yr^{-1}},\ \tau = 100\ \mathrm{yr} \end{cases}. \tag{6}$$

BNS mergers will produce gravitational waves, which can be observed by the Advanced LIGO/Virgo gravitational-wave detectors. Therefore, the fraction of magnetars born in BNS mergers can be constrained by gravitational-wave observations. Until 2020 February 1, the O3 observation of Advanced LIGO/Virgo was carried out for about 300 days. Only one event S190425Z, has a probability of more than 99% of being produced by BNS merger.[4] If the lifetime of repeating sources is 10 yr, considering the observation time $T = 300$ days and the detection range is 170 Mpc, the Advanced LIGO/Virgo may detect $33.08^{+5.75}_{-5.75}$ gravitational-wave events from BNS mergers, where the error is a Poisson error. If the lifetime is 100 yr, We expect Advanced LIGO/Virgo to detect $3.31^{+1.82}_{-1.82}$ GW events. Considering the most probable lifetime for magnetic activity is $\tau \simeq 20$ yr, the Advanced LIGO/Virgo can detect 16.54 ± 4.07 GW events in 300 days. If the detection of GW events satisfies the Poisson distribution, the probability that the number of observed gravitational-wave events is less than three is about 6×10^{-5}, which is almost impossible. Considering that one GW event from BNS merger was observed in the O3 observation, the fraction of repeating FRBs from BNS mergers is only 6%.

4. Discussion and Conclusions

In the above calculations, the NE2001 model of DMs for the Milky Way is used. Below, we consider the YMW17 model for the Milky Way (Yao et al. 2017). The values of $\mathrm{DM_{ex}}$ are comparable in the two models, except for FRB 180916.J0158+65. In this case, the value of $\mathrm{DM_{ex}}$ for FRB 180916.J0158+65 is only about 20 pc cm^{-3}, which is the lowest one. Compared with $\mathrm{DM_{ex}} = 149\ \mathrm{pc\,cm^{-3}}$ for this FRB in the NE2001 model, the corresponding critical distance d_c is much smaller than that in the NE2001 model. The above volumetric formation rate of repeating FRBs is conservative because some CHIME FRBs that have not been observed to repeat may be intrinsically repeating (Ravi 2019). Therefore, the derived lower limit is conservative and robust.

It is well known that BNS mergers are the leading model for short gamma-ray bursts, as confirmed by the first BNS gravitational-wave event GW170817/GRB 170817A (Abbott et al. 2017). If the merger product is a magnetar, it can potentially generate repeating FRBs. Therefore, monitoring the sites of short gamma-ray bursts is important to test this hypothesis. Our results suggest that magnetars powering FRBs may be from the core-collapses of massive stars, which also can produce long gamma-ray bursts. Some searches have been performed (Madison et al. 2019; Men et al. 2019); however, no FRB signal has been found. Therefore, future searches with more sensitive radio telescopes, i.e., FAST (Li et al. 2018), are important. Magnetars from core-collapse of massive stars and BNS mergers will have distinct host galaxy properties and spatial offset distributions (Wang et al. 2020). Therefore, the localization of a large sample of FRBs by the Australian Square Kilometre Array Pathfinder and Very Large Array could shed light on the formation channel of magnetars. The ongoing CHIME and Advanced LIGO/Virgo observations can refine the present analysis.

We thank the anonymous referee for constructive and helpful comments. This work is supported by the National Natural Science Foundation of China (grants U1831207 and 11703015).

ORCID iDs

G. Q. Zhang https://orcid.org/0000-0001-6545-4802
F. Y. Wang https://orcid.org/0000-0003-4157-7714

References

Abbott, B. P., Abbott, R., Abbott, T. D., et al. 2017, PhRvL, 119, 161101
Abbott, B. P., Abbott, R., Abbott, T. D., et al. 2018, LRR, 21, 3
Bannister, K. W., Deller, A. T., Phillips, C., et al. 2019, Sci, 365, 565
Beloborodov, A. M. 2017, ApJL, 843, L26
Beloborodov, A. M., & Li, X. 2016, ApJ, 833, 261
Berger, E. 2014, ARA&A, 52, 43
Caleb, M., Stappers, B. W., Rajwade, K., & Flynn, C. 2019, MNRAS, 484, 5500
Callister, T., Kanner, J., & Weinstein, A. 2016, ApJL, 825, L12
Cao, X.-F., Yu, Y.-W., & Dai, Z.-G. 2017, ApJL, 839, L20
Chatterjee, S., Law, C. J., Wharton, R. S., et al. 2017, Natur, 541, 58
CHIME/FRB Collaboration, Amiri, M., Bandura, K., et al. 2018, ApJ, 863, 48
CHIME/FRB Collaboration, Amiri, M., Bandura, K., et al. 2019a, Natur, 566, 235
CHIME/FRB Collaboration, Andersen, B. C., Bandura, K., et al. 2019b, ApJL, 885, L24
Cordes, J. M., & Chatterjee, S. 2019, ARA&A, 57, 417
Cordes, J. M., & Lazio, T. J. W. 2002, arXiv:astro-ph/0207156
Dai, Z. G., Wang, J. S., Wu, X. F., & Huang, Y. F. 2016, ApJ, 829, 27
Deng, W., & Zhang, B. 2014, ApJL, 783, L35
Fonseca, E., Andersen, B. C., Bhardwaj, M., et al. 2020, ApJL, 891, L6
Gehrels, N. 1986, ApJ, 303, 336
Geng, J. J., & Huang, Y. F. 2015, ApJ, 809, 24
Ioka, K. 2003, ApJL, 598, L79
James, C. W. 2019, MNRAS, 486, 5934
Kashiyama, K., & Murase, K. 2017, ApJL, 839, L3
Kulkarni, S. R., Ofek, E. O., Neill, J. D., Zheng, Z., & Juric, M. 2014, ApJ, 797, 70
Kumar, P., Shannon, R. M., Osłowski, S., et al. 2019, ApJL, 887, L30
Li, D., Wang, P., Qian, L., et al. 2018, IMMag, 19, 112
Lorimer, D. R., Bailes, M., McLaughlin, M. A., Narkevic, D. J., & Crawford, F. 2007, Sci, 318, 777
Madison, D. R., Agarwal, D., Aggarwal, K., et al. 2019, ApJ, 887, 252
Marcote, B., Paragi, Z., Hessels, J. W. T., et al. 2017, ApJL, 834, L8
Margalit, B., Berger, E., & Metzger, B. D. 2019, ApJ, 886, 110
Margalit, B., & Metzger, B. D. 2019, ApJL, 880, L15
Margalit, B., Metzger, B. D., Berger, E., et al. 2018, MNRAS, 481, 2407
Men, Y., Aggarwal, K., Li, Y., et al. 2019, MNRAS, 489, 3643
Metzger, B. D., Berger, E., & Margalit, B. 2017, ApJ, 841, 14
Murase, K., Kashiyama, K., & Mészáros, P. 2016, MNRAS, 461, 1498
Nicholl, M., Williams, P. K. G., Berger, E., et al. 2017, ApJ, 843, 84
Petroff, E., Hessels, J. W. T., & Lorimer, D. R. 2019, A&ARv, 27, 4
Platts, E., Weltman, A., Walters, A., et al. 2019, PhR, 821, 1
Popov, S. B., & Postnov, K. A. 2013, arXiv:1307.4924
Prochaska, J. X., Macquart, J.-P., McQuinn, M., et al. 2019, Sci, 366, 231
Prochaska, J. X., & Zheng, Y. 2019, MNRAS, 485, 648
Ravi, V. 2019, NatAs, 3, 928
Ravi, V., Catha, M., D'Addario, L., et al. 2019, Natur, 572, 352
Shull, J. M., & Danforth, C. W. 2018, ApJL, 852, L11
Shull, J. M., Smith, B. D., & Danforth, C. W. 2012, ApJ, 759, 23
Spitler, L. G., Scholz, P., Hessels, J. W. T., et al. 2016, Natur, 531, 202
Tendulkar, S. P., Bassa, C. G., Cordes, J. M., et al. 2017, ApJL, 834, L7
Thornton, D., Stappers, B., Bailes, M., et al. 2013, Sci, 341, 53
Totani, T. 2013, PASJ, 65, L12
Wang, F. Y., Wang, Y. Y., Yang, Y. P., et al. 2020, ApJ, 891, 72
Wang, J.-S., Yang, Y.-P., Wu, X.-F., Dai, Z.-G., & Wang, F.-Y. 2016, ApJL, 822, L7
Yamasaki, S., Totani, T., & Kiuchi, K. 2018, PASJ, 70, 39
Yao, J. M., Manchester, R. N., & Wang, N. 2017, ApJ, 835, 29
Zhang, B. 2014, ApJL, 780, L21
Zhang, B. 2017, ApJL, 836, L32
Zhang, B. 2020, ApJL, 890, L24
Zhang, G. Q., & Wang, F. Y. 2019, MNRAS, 487, 3672
Zhang, G. Q., Yu, H., He, J. H., & Wang, F. Y. 2020, ApJ, submitted

[4] https://gracedb.ligo.org/latest/